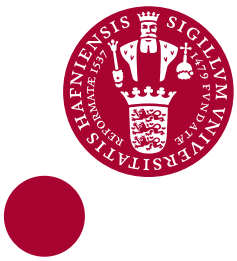

Importance of thorough conformational analysis in modelling transition metal-mediated reactions

Case studies on pincer complexes containing phosphine groups

Munkerup, Kristin; Thulin, Michael; Tan, Davin; Lim, Xiaozhi; Lee, Richmond; Huang, Kuo Wei

Published in:
Journal of Saudi Chemical Society

DOI:
10.1016/j.jscs.2019.07.005

Publication date:
2019

Document version
Publisher's PDF, also known as Version of record

Journal of Saudi Chemical Society (2019) **23**, 1206–1218

King Saud University

Journal of Saudi Chemical Society

www.ksu.edu.sa
www.sciencedirect.com

ORIGINAL ARTICLE

Importance of thorough conformational analysis in modelling transition metal-mediated reactions: Case studies on pincer complexes containing phosphine groups

Kristin Munkerup [a,1], Michael Thulin [b,1], Davin Tan [a], Xiaozhi Lim [a], Richmond Lee [a], Kuo-Wei Huang [a,*]

[a] *KAUST Catalysis Center & Division of Physical Science and Engineering, King Abdullah University of Science and Technology, Thuwal 23955-6900, Saudi Arabia*
[b] *Deparment of Computer Science, University of Copenhagen, Universitetsparken 1, 2100 Copenhagen Ø, Denmark*

Received 14 June 2019; revised 23 July 2019; accepted 25 July 2019
Available online 6 August 2019

KEYWORDS

Conformational analysis;
DFT;
Pincer;
Mechanism;
Rotamers

Abstract Advances in processing capabilities of computer clusters have allowed for the full modeling of organometallic complexes that previously would have been simplified to reduce computational cost. Increased feasibility of computational modeling offers new challenges, not only in terms of limitations of methods and theory, but attention should be paid to complexes that can exist in many conformations, as the appropriate choice of conformer may be easily overlooked. In this work a series of pincer complexes with isopropyl and cyclopentyl substituents have been chosen as examples to demonstrate the importance of conformational analysis. The complexes examined contain four isopropyl or cyclopentyl groups on phosphor atoms generating between 27 and 324 possible rotamers. The importance of conformational search in a mechanistic investigation is demonstrated with the CO_2 insertion into a nickel hydride bond of POCOP ^{i}Pr nickel hydride complex. Results show that the reaction energy profile can be both exergonic and endergonic depending on rotamer choice. Specifically, the POCOP^{iPr} Ni-formato complex product of the CO_2 insertion reaction had an energy difference between the lowest and highest energy rotamer as high as

* Corresponding author.
E-mail address: hkw@kaust.edu.sa (K.-W. Huang).
[1] These authors contributed equally.

Peer review under responsibility of King Saud University.

ELSEVIER Production and hosting by Elsevier

https://doi.org/10.1016/j.jscs.2019.07.005

16.8 kcal/mol. The significant energy differences between rotamers highlight the importance of thorough conformational analysis and should be taken into consideration when evaluating the energy profile of related reactions.

1. Introduction

Pincer complexes are a special class of organometallic complexes that carry pincer ligands [1–3]. Pincer ligands coordinate to the metal center in a meridional κ^3 fashion, allowing for stronger coordination, and varying modularity for the tuning of stereo-electronic properties [4–6]. Pincer complexes have been shown to exhibit intriguing catalytic activity in organic transformations [7–12], and computational tools such as density functional theory (DFT), are increasingly utilized to understand their reactivity by facilitating a better understanding of ligand properties, supporting experimental observations and gaining insight into mechanisms [13–18]. Information provided by theoretical studies has enabled the design of improved organometallic catalysts in order to achieve better activity, higher selectivity, and milder reaction conditions [19–21].

In an attempt to reduce computational cost, earlier theoretical studies simplified structures by truncating donor group substituents such as tertbutyl (^{t}Bu) or isopropyl (^{i}Pr) groups to either hydrogen or methyl groups [22–30]. However changing the alkyl ligand on for example a phosphine donor group also changes the stereoelectronic properties [31], activity, reactivity and even the reaction mechanism of a given metal complex [32–38]. The constant improvements in processing capabilities of computer clusters eliminates the need to truncate structures for shorter computation time, thereby allowing for the full modeling of structures [38–40]. As highlighted in recent work by Baik and co-workers, modern computational software has made it easier for non-specialists to use computational tools, but also increases the risk for misinterpretation of results due to a lack of deep understanding of how the computational software computes the molecular energies and properties [41].

From introductory organic chemistry, we learn about Newman projections as a useful tool to look at rotamer conformations around two sigma bonded tetrahedral atom centers [42]. One of the first examples of Newman projections that most chemists encounter is that of butane and the rotation around the C2–C3 single bond as can be recalled from Fig. 1: the largest groups (e.g. methyl) should be in the *anti* position in order to afford the lowest energy conformer. With every 60 degrees rotation around the CCCC dihedral angle in butane a high energy eclipsed conformer will be generated followed by a local minima gauche conformer until the 360-degree rotation returns butane to the initial global minimum anti conformer. Similar to butane, pincer metal complexes with phosphine alkyl groups such as isopropyl (^{i}Pr) and cyclopentyl (^{c}Pe) substituents shown in Fig. 2 have a different rotamer generated with every 120-degree rotation. However, optimization of individual rotamers does not adjust a higher-energy rotamer (local minimum) to the lowest-energy rotamer (global minimum), i.e.: each rotamer typically dwells in its own potential energy well [41]. As a result, it can be challenging to locate the appropriate structure for a theoretical study.

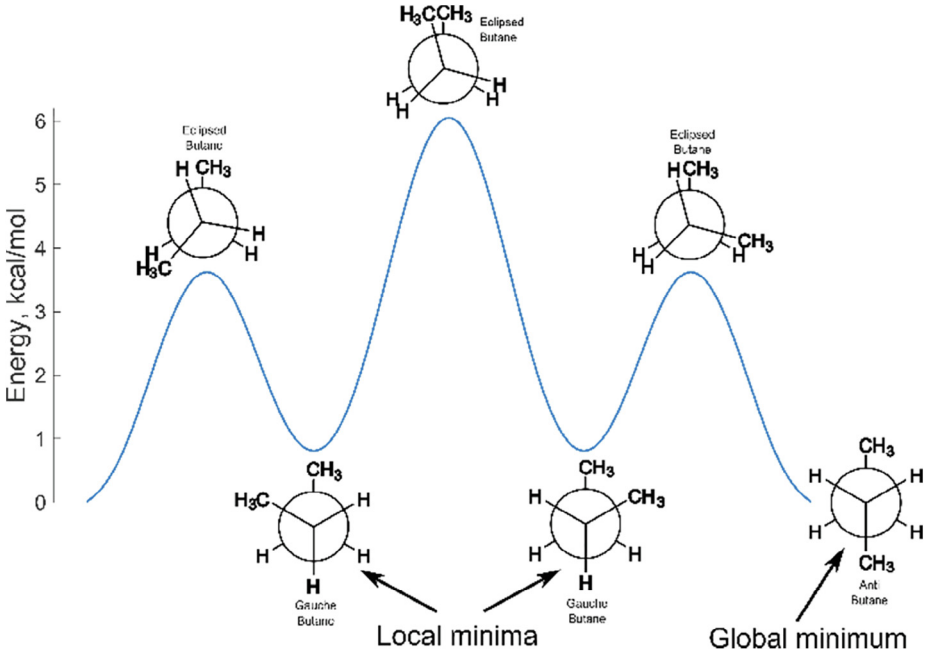

Fig. 1 Potential energy diagram of the butane rotation around the C2–C3 bond. Newman projections are drawn at each minimum and maximum.

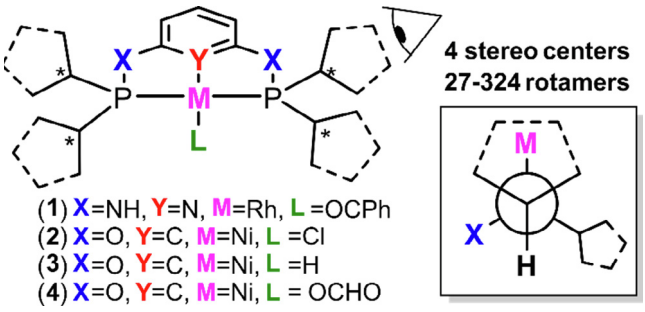

Fig. 2 Pincer complexes with chiral phosphine centers containing isopropyl and cyclopentyl groups included in this study.

In organic catalyzed transformations multiple conformers and modes of attack from a substrate are considered in mechanistic investigations [43–48], but this is in sharp contrast to computational studies involving the full modeling of organometallic pincer complexes bearing stereogenic phosphine groups where rotamers are often not mentioned [40,49–60]. In fact, only two examples could be found discussing conformers, one is of an asymmetric pincer complex that had methyl, cyclohexyl phosphine arms [61], the other example involves a pincer complex bearing stereogenic phosphine isopropyl groups where conformers were evaluated only in critical energy barriers of the calculated mechanism [62]. This is why we see it necessary to reiterate the importance of the conformational search in organometallic complexes, using a set of pincer complexes as examples. The common approach is to model the metal complexes in question after the structure obtained from single crystal X-ray diffraction analysis [50–51,63]. While this is a reasonable approach, crystal structures are not always available and there can be exceptions where the molecular structure obtained from the single crystal analysis does not correspond to the most stable conformer in calculations [64,65]. There are a few recent articles highlighting the significance of conformational search in metal complexes; one example was on cobalt complexes with cyclam ligand derivatives and the other on palladium complexes with diphosphine ligands [66–68]. Both applied the Monte Carlo Multiple Minimum (MCMM) conformational search method to identify the most stable conformers and in case of the palladium diphosphine complexes, a Gibbs free energy span of 11.4 kcal/mol was found between highest and lowest energy conformer. Although there is a general consensus in the field of chemistry that conformers should be considered, it is not commonly practiced in computational studies on organometallic pincer complexes. Furthermore, identifying all the rotamers reveals which ones are energetically available under the given reaction conditions thereby providing important information for understanding and calculating the mechanism, as the lowest energy conformer might not always be the one to facilitate observed reactivity. Thus, for a deeper investigation into the roles that rotamers play in locating the global minimum and in calculating reaction pathways of pincer complexes with ^{i}Pr and ^{c}Pe substituents on phosphines, a closer examination of all rotamers derived from four pincer complexes has been carried out. In the following we will investigate all the rotamers for complexes **1**–**4** in Fig. 2 with DFT and conclude with an example of rotamer influence on relative energy in the potential energy profile of CO_2 insertion into a nickel hydride (complexes **3** and 4) [33,69–72]. A new software developed in our group for the purpose of generating rotamers is introduced. The software reads a typical Gaussian input file with connectivity and the user can choose dihedral angles to be rotated and the software generates all combinations of the specified rotations. The importance of conformational search is reflected in the several softwares available which can automatically search for low energy conformers, such as for example the free software Balloon, CONFAB, Frog2, and RDKit and commercial software MOE, ConfGenX, OMEGA, and many others [73–75]. These softwares mostly rely on using semi-empirical methods or molecular mechanics but are not widely applicable to transition metal complexes. [76]. The GenRot software [100] provided in this work differs from the mentioned softwares, as it does not try to find low energy conformers, it simply takes a Gaussian type XYZ input, asks the user to define dihedral angles and degree of rotation and generates the XYZ coordinates of all possible rotamers in an easy and simple way.

2. Computational details

DFT calculations were performed with the Gaussian 09 program version D.01 [77]. All the input files for Gaussian were generated with the GenRot software, [100] a software developed by us specifically for the purpose of generating rotamers of pincer complexes. The GenRot software works for all types of molecules with dihedral angles. A description and documentation of the GenRot software is provided in Supporting information.[†] Becke's three parameter functional with the nonlocal Lee-Yang-Parr correlation functional (B3LYP) [78] theory was applied. As this work aims to be a proof of concept and not reproduce observed energies nor calculate mechanisms for understanding reactivity, the B3LYP functional has been chosen as it is quick, and has been shown to perform well in geometry optimizations and reproducing C–H activation barriers [79–80]. Cavallo and coworkers have shown, that there is no one functional that performs well for all metals and ligands [76], and the choice of DFT functional and effective core potential (ECP) should be carefully chosen based on benchmark studies in the literature and evaluated on a case by case basis [81–82]. In this work, the LANL2DZ basis set including valence basis set with the Hay and Wadt ECP [83–85] was used for Ni and Rh atom, and 6-31G(d) Pople basis set for the rest of the atoms [86–89]. Crystal structures of complexes **1**, **2** and **4** are shown in supporting information (Figs. S1–S3) and were optimized to a minimum before being loaded into the GenRot software and all the other rotamers were generated. Optimization convergence was performed using verytight convergence criteria in the OPT and SCF protocols together with an ultrafine grid on integrals. Frequency calculations were performed on optimized structures to ensure that a minimum had been reached. All transition states were confirmed to having only one imaginary frequency. The lowest energy conformer is related to the lowest conformer found by screening of rotamers, as there is no straightforward protocol to calculate the true lowest energy conformer. In the following when we indicate global minimum, we refer to the lowest energy conformer out of all the conformers that have been considered. It can

however not be guaranteed that it is the true global minimum. All energies stated in the following are Gibbs free energies in kcal/mol.

3. Result and discussion

3.1. PN^3P^{-cPe}-Rh(I) complex 1

The PN^3P^{-cPe}-Rh(I) complex **1** was first synthesized by our group and facilitates the selective carbonylation of benzene to benzaldehyde [90]. Complex **1** has four ^{c}Pe groups where a new rotamer is generated with every 120-degree rotation around the P–C single bond leading to 81 rotamers (see Fig. S4). More rotamers can be generated if all the conformations of the ^{c}Pe groups are included, however, it has been shown in a study on tetrahydrofuran that the predicted relative energy of all the possible conformers is highly dependent on the prediction model used, thus making such an investigation too broad [91]. Complex **1** has one mirror plane (Fig. S5) reducing 81 rotamers to 45 unique rotamers. However, as can be seen from Fig. S6 some of the symmetry-related pairs will not necessarily have the exact same energy. The biggest energy difference found between symmetry-related pair of rotamers being 1.6 kcal/mol between **Rhodium_12** and **Rhodium_56** with the main structural difference between them being the conformations of the ^{c}Pe groups (Fig. S7). All the rotamers exhibit a planar pincer configuration and all relative energies are given in Table S1 and the position of the benzaldehyde ligand will change with the rotation of the ^{c}Pe groups (Fig. S7). The global minimum corresponds to the crystal structure (**Rhodium_30**) and the highest local minimum corresponds to **Rhodium_19** with a relative energy between them of 11.0 kcal/mol (Fig. 3A). By drawing the Newman projections

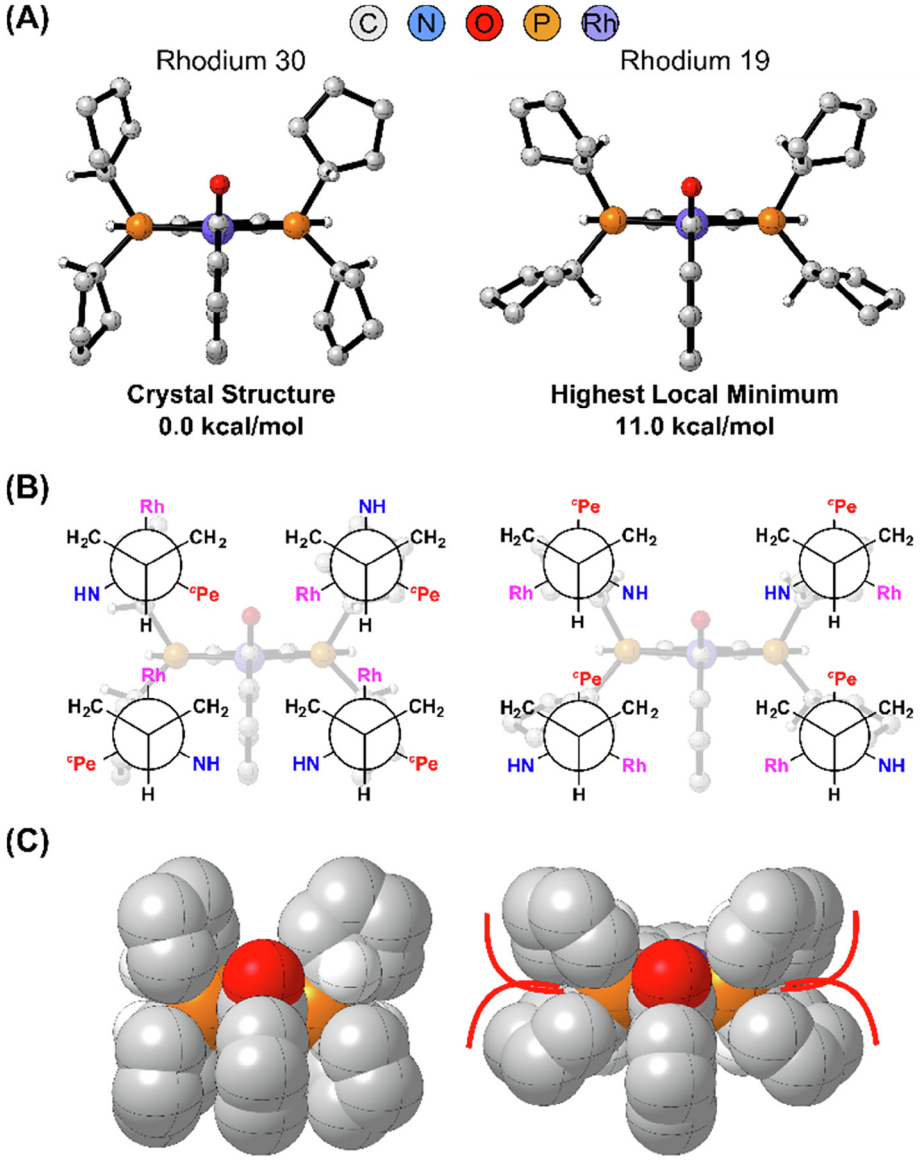

Fig. 3 (A) DFT optimized Crystal structure (the global minimum) and highest local minimum structure of complex 1 together with relative energies given in kcal/mol. (B) Newman projections of each individual ^{c}Pe group in the global and local minima structure depicted in (A). (C) VdW radii representation of global and local minima from (A).

(note, always with proton drawn down for easy comparison) for each ^{c}Pe group in the highest local minimum and global minimum of pincer complex **1** (Fig. 3B) it is straightforward to rationalize the high and low energies; in the global minimum the more bulky ^{c}Pe group is *syn* to the small hydrogen, while in the highest local minimum the ^{c}Pe group is *anti* to the hydrogen and between the two CH_2 groups, meaning the ^{c}Pe groups are *syn* and the steric induced by this *syn* configuration is illustrated in the VdW radius representation in Fig. 3C. Thus, considering only the global and highest local minimum of **1,** the rational stating that the lower energy rotamer is obtained with the bulky groups in an anti position to each other can be applied to complex **1**. Furthermore, the four lowest energy conformers all have a relative energy within 1 kcal/mol and have the ^{c}Pe group syn to the hydrogen while the four highest energy conformers have a relative energy above 8.5 kcal/mol with three or four out of four ^{c}Pe groups anti to the hydrogen (Fig. S8). While it is straightforward to find the highest energy conformers of complex **1** by having as many possible ^{c}Pe groups anti to H as possible, it is not straightforward to find the global minimum as there are many rotamers that have ^{c}Pe in the syn position to H. Therefore a conformational analysis of rotamers is still necessary in order to ensure the global minimum has been found.

3.2. POCOP^{iPr}-NiCl complex 2

The next complex studied is the square-planar POCOP^{iPr}-Ni(II)-chloride complex **2** first prepared by Zargarian and co-workers [69]. This complex is an important synthetic precursor for other complexes that have been developed and used as catalysts in reactions such as the addition of amines and phenols to acrylonitrile derivatives and carbon dioxide reduction [71,92–95]. A total of 27 unique rotamers are found for complex **2** (Fig. S9), but 81 rotamers were generated with the GenRot software and optimized. An energy difference of 1.0 kcal/mol could be found between symmetry-related rotamer duplicates NiCl_31, NiCl_39, and NiCl_67, which arises from differences in the rotation in the ^{i}Pr groups (Fig. S10). The optimized structures have a planar geometry around the nickel center and the arrangement of the ^{i}Pr groups in the global minimum are diagonally equivalent with a mirror plane in the Cl–Ni–C plane. The energy difference between the global minimum and the highest local minimum is 8.6 kcal/mol (Fig. 4) and the majority of the rest of the rotamers are between 1 and 5 kcal/mol higher in energy than the global minimum.

The experimentally obtained structure of **2** from single crystal X-ray diffraction analysis was only 0.3 kcal/mol higher in energy relative to the global minimum. Interestingly the highest global minimum of NiCl has all four ^{i}Pr groups anti to the proton, showing here that the ^{i}Pr groups induce the largest steric therefore, in this case, it is straightforward to predict and avoid the high energy rotamer, however, as in the case of complex **1**, the lowest energy conformer is not easily predicted again emphasizing the importance of conformational analysis.

3.3. POCOP^{iPr}-NiH complex 3

The fourth complex in our case study is the POCOP^{iPr}-Ni(II)-hydrido complex **3** reported by Guan and co-workers and was recently demonstrated to catalyze the dehydrogenative coupling of aldehydes with alcohols [70,96]. It was not possible to find a crystal structure for this complex, therefore the structure of complex **2** was used as a model to create the structure of complex **3** by replacing the chloride with a hydride. Like complex **2** this complex has 27 unique rotamers but 81 rotamers were optimized. The largest energy difference between rotamer duplicate pair is 0.8 kcal/mol between NiH_5 and NiH_63 and arises from a difference in the rotation in the ^{i}Pr groups (Fig. S12). Our calculations reveal that the difference in energy between the highest local minimum and global minimum (Fig. 5) is 6.9 kcal/mol. The global minimum structure of complex **3** has a planar and symmetrical geometry, which is consistent with the molecular structures of relevant pincer complexes in the literature[5,54,97–98].

The spatial orientations of the ^{i}Pr groups in the highest local minimum and global minimum are the same in complex **2** and complex **3** which suggests that the spatial orientations of the ^{i}Pr groups are not sensitive to the nature of the size of the single atom ligand (e.g. H or Cl) closest to the isopropyl

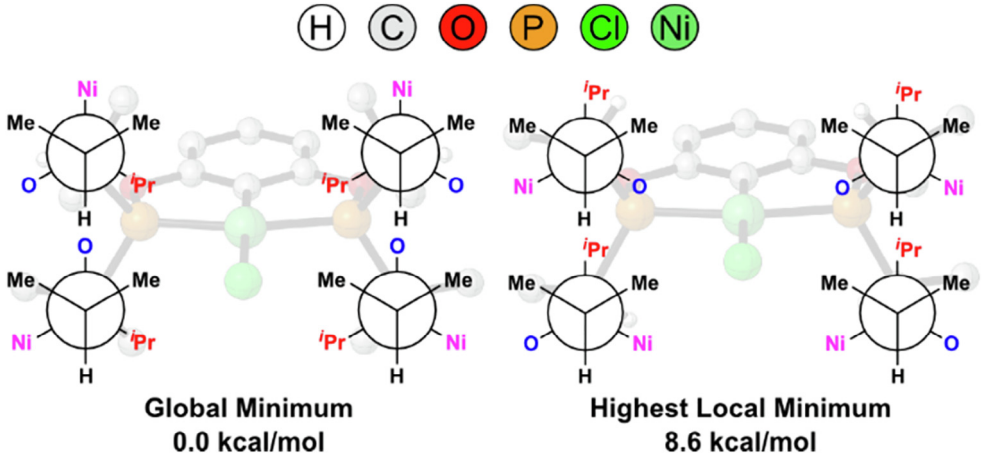

Fig. 4 Structural rotamers of highest local minimum and global minimum of the Zagarian's POCOP^{iPr}-Ni(II)-chloride complex **2**. C–H hydrogens removed for clarity.

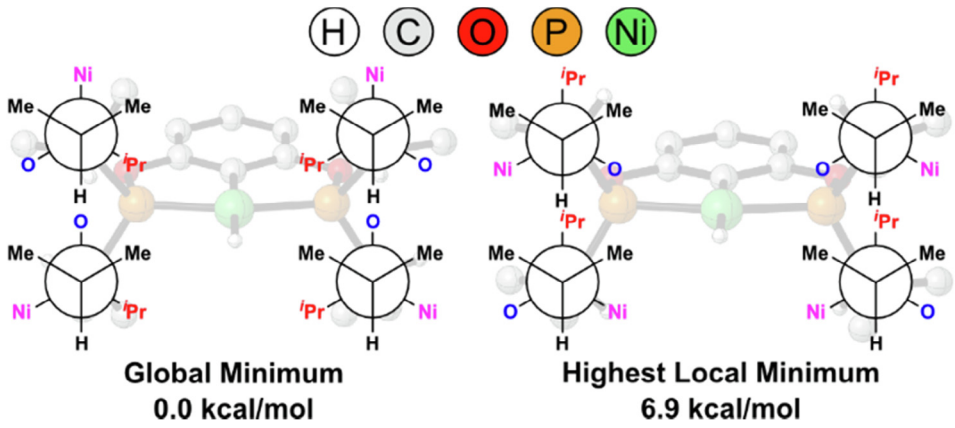

Fig. 5 Structural rotamers of the highest local minimum and global minimum of Guan's POCOP^{iPr}-Ni(II)-hydrido complex 3. C–H hydrogens removed for clarity.

groups. However, as we will see in the next section, increasing the size of the ligand from one atom to a molecular group will have a significant effect on the relative energy.

3.4. POCOP^{iPr}-Ni complex ***4***

POCOP^{iPr}-Ni(II)-formato complex **4** reported by Guan and co-workers [71] has proved to be particularly challenging as there is a total of 324 unique rotamers of the complex. This can be rationalized by the following:

- Each ^{i}Pr group creates a unique spatial rotamer with every 120-degree rotation, thereby generating 81 (3^4) conformations.
- The formato group can be parallel or perpendicular to the plane of the pincer ligand, with the hydrogen *syn* or *anti* to the nickel center, thereby generating four conformations for each of the 81 conformations, totaling to 324 rotamers.

In order to accurately locate the structure of the global minimum, we proceeded to identify all 324 rotamers. The global minimum is found in the set of rotamers with the formato ligand parallel to the plane of the POCOP^{iPr} pincer ligand, and the formato hydrogen *anti* to the nickel center.

The relative highest local minimum with the highest energy was found to belong in the set of rotamers with the formato ligand perpendicular to the plane of the POCOP^{iPr} pincer ligand, and the formato hydrogen *syn* to the nickel center (Fig. 6). The energy difference between them was found to be a staggering 16.8 kcal/mol! Within each configuration of the formato ligand, the energy difference between lowest and highest local minima ranges from 8.4 to 13.6 kcal/mol.

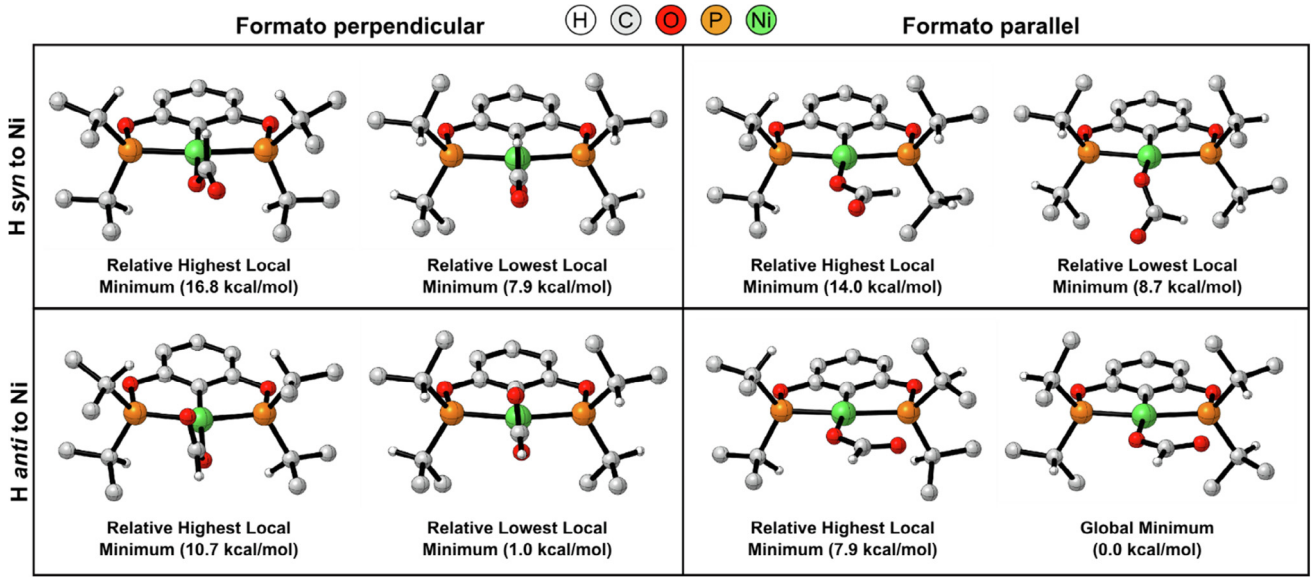

Fig. 6 Structural rotamers of the Guan's POCOP^{iPr}-Ni(II)-formato complex **4**. The 324 rotamers are divided into four sets: H *syn* to Ni and formato perpendicular (top left), H *syn* and formato parallel (top right), H *anti* and formato perpendicular (bottom left) and H *anti* and formato parallel (bottom right). The relative highest and lowest local minimum structure is shown for each set along with relative energies given in kcal/mol.

A comparison of the energy distribution of rotamers within each set of rotamers (Chart 1) shows that each set of energy distribution resembles a normal, or Gaussian, distribution. For the two sets of rotamers with the formato hydrogen *anti* to the nickel center and the one set with H *syn* to Ni and the formato group perpendicular, most of the rotamers were observed to be found within 7 kcal/mol of their relative lowest local minima (Chart 1, blue, grey and yellow data). On the other hand, the rotamer set with the formato hydrogen *syn* to the Ni center and the formato group parallel most of the rotamers are 3–10 kcal/mol higher in energy than the lowest local minimum (Chart 1, orange data) and a lot of the rotamers in this set optimize to different structures, for example, H becoming anti and the formato group becoming perpendicular (Table S8). This shows that the set of rotamers with the formato ligand perpendicular to the pincer plane are energetically favored (Chart 1) and the formato hydrogen is small enough for the formato ligand to get past the bulky ^{i}Pr groups while the formato oxygen atom in the set of rotamers with the formato ligand parallel and H *anti* is too large and the formato cannot get past the ^{i}Pr groups and therefore stays parallel to the pincer plane. When each set of rotamers with different spatial orientations of the formato ligand were compared, the relative energy of the rotamers depended more on whether the formato hydrogen was *syn* or *anti* to the nickel center and less on whether the formato ligand was perpendicular or parallel to the plane of the POCOP^{iPr} pincer ligand. In this case, the arrangements of the ^{i}Pr substituents and the resulting energies of the rotamers seem to depend strongly on the exact spatial orientation of the formato ligand.

Even though the ligand is the same and only its spatial arrangement is varied, this difference in the orientation of the formato ligand results in sets of rotamers that show large differences in energy. This demonstrates the dependence of the rotamers' stabilities on the steric influences of the formato ligand as well as that of the ^{i}Pr substituents on the pincer ligand.

When the calculated structure of the global minimum and the experimentally obtained structure from single crystal X-ray diffraction analysis (Fig. S14) were compared, it was observed that they both belong in the set of rotamers with the formato ligand parallel to the plane of the POCOP^{iPr} pincer ligand and the formato hydrogen *anti* to the nickel center. The two structures were not identical, with two ^{i}Pr substituents differing in their rotational orientation. This could be attributed to the different spatial requirements for the greatest stability of the complex in a single crystal versus the gaseous state. The X-ray crystal structure had a small energy difference of +0.4 kcal/mol compared to the calculated global minimum structure.

*3.5. Reaction energy profile for CO_2 insertion into a Ni–H bond of **3***

From these findings, it is evident that the spatial arrangement of the ^{i}Pr substituents can influence the relative energy of pincer complexes to a large degree. The rotamers can have significant energy ranges which can represent misleading conclusions in mechanistic studies. For example, a higher-energy rotamer could be mistaken for an energetically disfavored complex structure but if the true global minimum were used, the results could be very different. Therefore, the spatial arrangement of the ^{i}Pr substituents can influence the choice of complex structures and also the calculated energy profiles of reactions directly. The large range in the energy difference observed above between rotamers demonstrates the significance of a rigorous conformational analysis. It is thus essential to identify all possible rotamers for systems with ^{i}Pr or ^{c}Pe groups in order to locate the true global minimum before embarking on mechanistic studies. This is especially important when establishing the energy profile of a reaction of interest.

With this concept in mind, we carried out a thorough study for the process of carbon dioxide insertion into the Ni-H bond of the POCOP^{iPr}-Ni(II)-hydrido complex **3**. The energy difference between the highest relative transition state energy structure and the lowest relative transition state energy structure (Fig. 7) is 9.1 kcal/mol, an energy difference large enough to render a mechanism implausible rather than plausible in a mechanistic study. An interesting observation from the highest relative transition state energy structure in Fig. 7 is that all the hydrogens on the isopropyl groups are pointing in towards the metal center which intuitively should leave an open cavity for

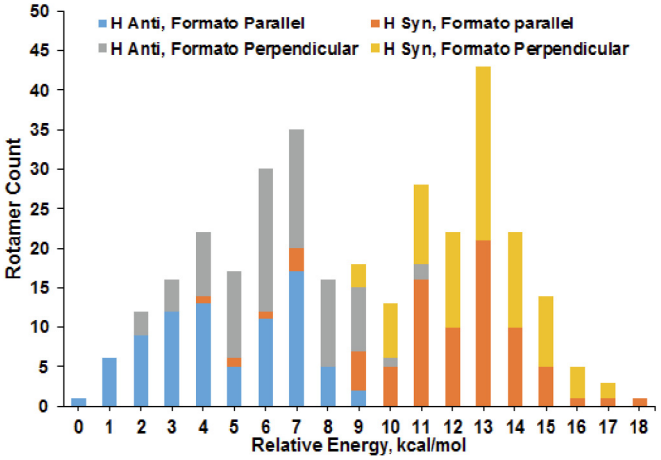

Chart 1 Energy distribution of the rotamers of **4**. H *anti* and formato parallel (blue), H *anti* and formato perpendicular (grey), H *syn* and formato parallel (orange) and, H *syn* and formato perpendicular (yellow).

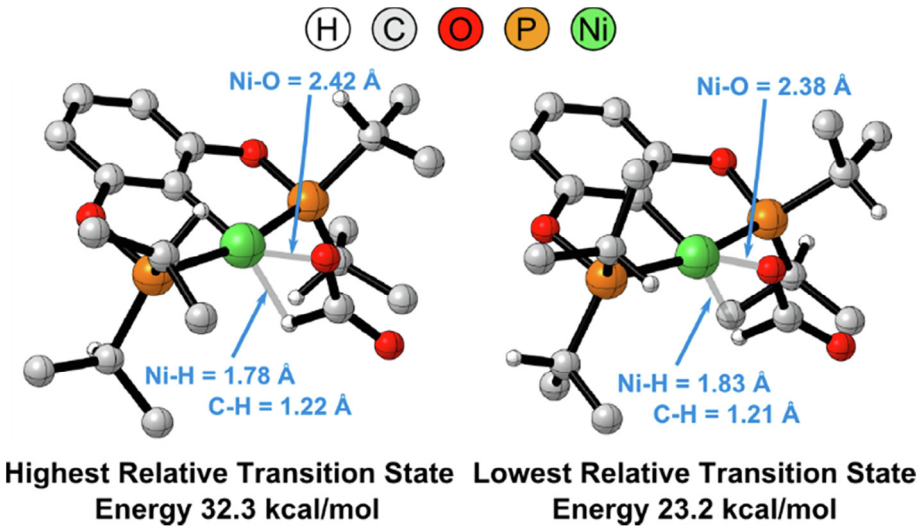

Fig. 7 Highest energy and lowest energy transition state structures for the reduction of CO_2 by POCOP^{iPr}-Ni(II)-hydrido complex **3**.

the carbon dioxide to be reduced but the steric effect from the clashing methyl groups has a greater effect on the relative energy.

After computing all the possible rotamers, we were able to create the relative free energy profile for the reduction of carbon dioxide by complex **3** (Fig. 8). 81 possible transition state geometries were evaluated for the hydride transfer process since the transfer from Ni to C only occurs to afford the "H *syn* to Ni" rotamers of the formato complex **4**.

To further highlight the significance of choosing the true global minimum when constructing an energy profile, the pathway **C** → **TS$_{CD}$** → **D** comprising of the global minima of the starting material, transition state and product structures, as shown as the blue line in Fig. 8, illustrated an exergonic process of −6.3 kcal/mol. This is in agreement with experimental results whereby the reaction occurred readily under room temperature and at low CO_2 pressure. If highest local minima structures for the transition state (**TS$_{AB}$**) and product (**B**) were chosen, the reaction would have to overcome a higher activation barrier of +25.4 kcal/mol and the reaction would have been endergonic (+3.6 kcal/mol). The grey shaded area depicts the range of all possible thermodynamic pathways for any arbitrarily chosen set of rotamers in the reaction profile between the highest local minima and global minima of all the structures.

The lowest energy conformer of **3** is NiH_8 which has relative energy of 0.0, and, depending on the mode of approach by the CO_2 molecule, there are two possible transition states, namely the lowest energy transition state TS_44 with a relative energy of 23.2 and TS_0 with a relative energy of 23.8 kcal/mol

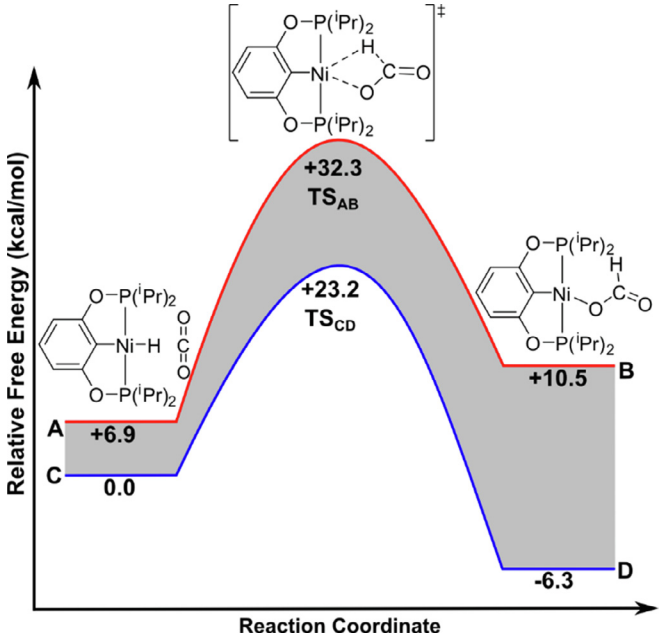

Fig. 8 Relative free energy profile for the reduction of CO_2 by POCOP^{iPr}-Ni(II)-hydrido complex **3**.

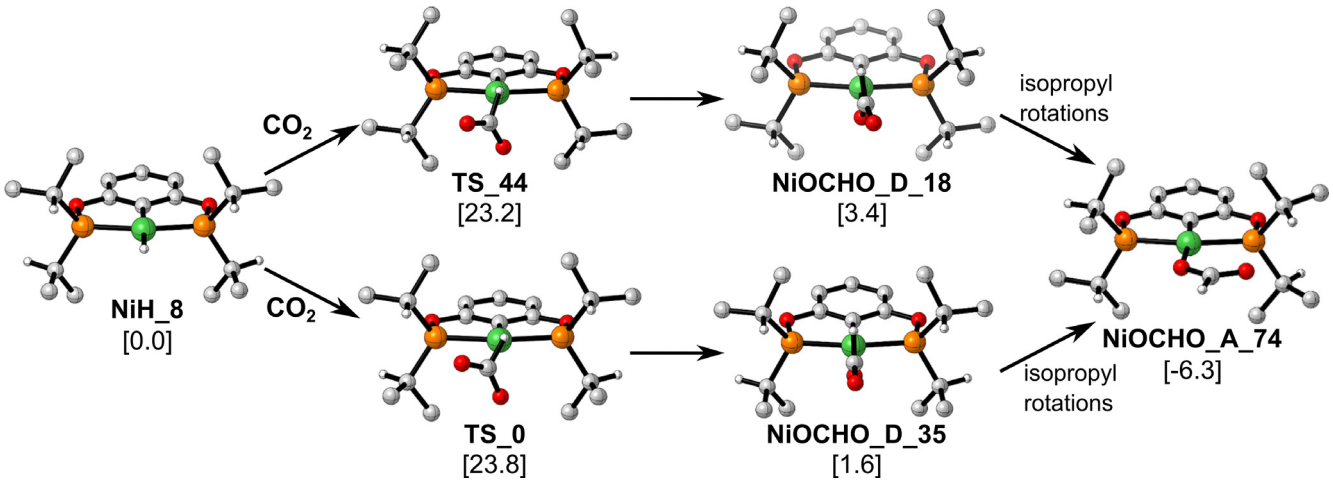

Fig. 9 Rotamers with energy given in kcal/mol shown in brackets.The lowest energy rotamer of complex **3**, NiH_8 can lead to two different transition states depending on which side the CO_2 approaches from. The two possible transition states are among the lowest energy transition states (TS_44 and TS_0). These transition states will become NiOCHO_D rotamers 18 and 35 which again are among the lowest energy rotamers of that set. These will then rearrange to become NiOCHO_A_74, the global minimum (given that the rotational barrier is not too big).

(Fig. 9). These two transition states will lead to NiOCHO_D_18 with a relative energy of 3.4 kcal/mol and NiOCHO_D_35 with a relative energy of 1.6 kcal/mol respectively as can be seen in Fig. 9. Based on the rotamer of the lowest NiH complex **3**, the reaction energy profile is endergonic (before rearrangement to global energy minimum of complex **4**).

This case study clearly demonstrates the need for evaluating all possible rotamers in order to elucidate and determine the mechanistic pathway of the reaction under theoretical studies.

3.6. Molecular Boltzmann partition weights

While evaluating all conformers is important for identifying low and high energy conformers not all of them have to be considered in a mechanistic study, only the rotamers which will be thermally accessible at a given temperature needs to be considered. In order to evaluate which rotamers will be thermally accessible at room temperature the molecular Boltzmann partition function, p_i, has been calculated for each rotamer, i, in each of the pincer complexes **1**–**4** as well as the transition states (TS) from the CO_2 insertion into the nickel hydride bond of complex **3** [44]. The molecular Boltzmann partition function quantifies the occurrence of each rotamer and is given by Eq. (1),

$$p_i = \frac{\exp\left(-\frac{E_i}{k_b T}\right)}{\sum_{j=1}^{N} \exp\left(-\frac{E_j}{k_b T}\right)} \quad (1)$$

where k_b is the Boltzmann constant, E_i the relative Gibbs free energy of rotamer i, and T the temperature in Kelvin and N the number of rotamers. As mentioned previously 81 rotamers were optimized for complex **1**–**4** despite some of them being related by symmetry operations and all these 81 rotamers have been included in calculating the molecular Boltzmann partition function as most of the supposed duplicates actually do not have the exact same energy. The partition functions for each rotamer of each complex **1**–**4** and TS are shown in Fig. 10, rotamers with a partition function greater than 0.1245 are marked with green, while rotamers with a partition function below 0.1245 but higher than 0.01 are yellow and rotamers with partition function lower than 0.01 have been given a red color. The cutoff values of p_i were chosen such that at least one rotamer would be in green for each set of rotamers in Fig. 10. In order to be able to reproduce experimentally observed energy barriers and product compositions with computational mechanistic studies, all the rotamers which have a

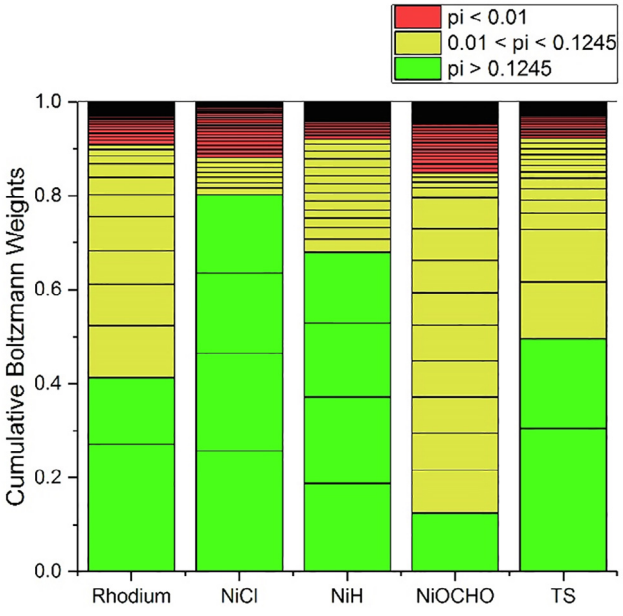

Fig. 10 Cumulative Boltzmann weights of all rotamers. 81 rotamers were considered for complexes **1** (rhodium), **2** (NiCl), **3** (NiH) and TS and 324 rotamers considered for NiOCHO complex **4**. Each entry is colored according to their partition function value; p_i higher than 0.1245 (green), p_i higher than 0.01 and less than 0.1245 (yellow) and p_i less than 0.01 (red).

large partition function should be considered. Evaluating the Boltzmann partition functions for each conformer becomes especially important if there is a question of kinetic versus thermodynamic control in a reaction [44].

4. Conclusion

In summary, we have located the global and local minima for complexes **1** to **4** by calculating every possible unique rotamer and established a reaction energy profile for carbon dioxide reduction by **3**. Through this process, we have shown that the energy difference between a single set of rotamers could be as large as 16.8 kcal/mol as shown in complex **4**, thereby demonstrating that rigorous conformational analysis of the complexes involved in a reaction is essential for an accurate assessment of a reaction profile. Despite using verytight SCF convergence criteria, symmetry related pairs of rotamers that are supposed to be degenerate may have a relative energy difference as high as 1.6 kcal/mol as shown in complex **1**, **2** and **3**. High energy conformers have bulky groups in *syn* position and low energy conformers have bulky groups in *anti* position as can be easily realized by drawing Newman projections of each stereogenic center. However, it is not straightforward to predict which rotamer will be the global minimum. Crystal structures serve as good guesses for a computational study but it is not the rule as seen in complex **4** and crystal structures are not always available as was the case for complex **3**. Therefore identifying all rotamers should still be done using DFT and each rotamer Boltzmann weight evaluated. Using cheaper methods such as force field and semi-empirical for the evaluation of relative energies does not yield consistent results as mentioned in the literature [76]. Finally, we have developed and used a new software, GenRot, which takes a Gaussian input file and dihedral angles as input to automatically generate all the Gaussian input files for each rotamer. This software is now available to the scientific community free of charge on the KAUST repository [100].

This work re-emphasizes and adds to the report by Lledós and co-workers with regard to the importance and necessity of conformational analysis for the appropriate choice of rotamer prior to any further mechanistic study, with particular relevance to computational studies involving organometallic pincer complexes with ^{i}Pr and ^{c}Pe substituents. Our case studies demonstrate the important but often neglected roles that rotamers play in computational investigations of organometallic compounds and their reactivity. While this study has focused on stereogenic pincer complexes, the conclusions should apply to other organometallic complexes with a diverse conformational space.

Declaration of Competing Interest

The authors declare that they have no known competing financial interests or personal relationships that could have appeared to influence the work reported in this paper.

Acknowledgments

The authors acknowledge the service of Ibex and Shaheen 2 High Performance Computing Facilities and financial support from King Abdullah University of Science and Technology (KAUST).

Appendix A. Supplementary data

Supplementary data to this article can be found online at https://doi.org/10.1016/j.jscs.2019.07.005.

References

[1] D. Morales-Morales, C.M. Jensen, The Chemistry of Pincer Compounds, Elsevier, 2007.
[2] G.V. Koten, Organometallic pincer chemistry, in: D.M. Gerard van Koten (Ed.), Top. Organomet. Chem., Springer, 2013, pp. 1–20.
[3] K.J. Szabó, O.F. Wendt, Pincer and Pincer-type Complexes: Applications in Organic Synthesis and Catalysis, Wiley-VCH Verlag GmbH & Co, KGaA, 2014.
[4] W. Leis, H.A. Mayer, W.C. Kaska, Cycloheptatrienyl, alkyl and aryl PCP-pincer complexes: ligand backbone effects and metal reactivity, Coord. Chem. Rev. 252 (15–17) (2008) 1787–1797.
[5] Z. Huang, M. Brookhart, A.S. Goldman, S. Kundu, A. Ray, S. L. Scott, B.C. Vicentec, Highly active and recyclable heterogeneous iridium pincer catalysts for transfer dehydrogenation of alkanes, Adv. Synth. Catal. 351 (2009) 188–206.
[6] A. Kumar, T. Zhou, T.J. Emge, O. Mironov, R.J. Saxton, K. Krogh-Jespersen, A.S. Goldman, Dehydrogenation of n-alkanes by solid-phase molecular pincer-iridium catalysts. High yields of α-olefin product, J. Am. Chem. Soc. 137 (31) (2015) 9894–9911.
[7] J. Choi, A.H.R. MacArthur, M. Brookhart, A.S. Goldman, Dehydrogenation and related reactions catalyzed by iridium pincer complexes, Chem. Rev. 111 (3) (2011) 1761–1779.
[8] C. Gunanathan, D. Milstein, Bond activation and catalysis by ruthenium pincer complexes, Chem. Rev. 114 (24) (2014) 12024–12087.
[9] H. Li, B. Zheng, K.-W. Huang, A new class of PN^3-pincer ligands for metal-ligand cooperative catalysis, Coord. Chem. Rev. 293 (2015) 116–138.
[10] C. Guan, D.-D. Zhang, Y. Pan, M. Iguchi, M.J. Ajitha, J. Hu, H. Li, C. Yao, M.-H. Huang, S. Min, J. Zheng, Y. Himeda, H. Kawanami, K.-W. Huang, Dehydrogenation of formic acid catalyzed by a ruthenium complex with an N, N′-diimine ligand, Inorg. Chem. 56 (1) (2017) 438–445.
[11] H. Li, Y. Wang, Z. Lai, K.-W. Huang, Selective catalytic hydrogenation of arenols by a well-defined complex of ruthenium and phosphorus-nitrogen PN^3–pincer ligand containing a phenanthroline backbone, ACS Catal. 7 (7) (2017) 4446–4450.
[12] H. Li, T.P. Gonçalves, D. Lupp, K.-W. Huang, PN^3(P)-pincer complexes: cooperative catalysis and beyond, ACS Catal. (2019) 1619–1629.
[13] K.W. Huang, D.C. Grills, J.H. Han, D.J. Szalda, E. Fujita, Selective decarbonylation by a pincer PCP-rhodium(I) complex, Inorg. Chim. Acta 361 (11) (2008) 3327–3331.
[14] N. Fey, The contribution of computational studies to organometallic catalysis: descriptors, mechanisms and models, Dalton Trans. 39 (2) (2010) 296–310.
[15] I. Osadchuk, T. Tamm, M.S.G. Ahlquist, Theoretical investigation of a parallel catalytic cycle in CO_2 hydrogenation by (PNP)IrH_3, Organometallics 34 (2015) 4932–4940.
[16] J.V. Obligacion, S.P. Semproni, I. Pappas, P.J. Chirik, Cobalt-catalyzed C(sp^2)-H borylation: mechanistic insights inspire catalyst design, J. Am. Chem. Soc. 138 (33) (2016) 10645–10653.
[17] T.P. Gonçalves, K.-W. Huang, Metal-ligand cooperative reactivity in the (pseudo)-dearomatized PN^x(P) systems: the influence of the zwitterionic form in dearomatized pincer complexes, J. Am. Chem. Soc. 139 (38) (2017) 13442–13449.

[18] J. Masdemont, J.A. Luque-Urrutia, M. Gimferrer, D. Milstein, A. Poater, Mechanism of coupling of alcohols and amines to generate aldimines and H_2 by a pincer manganese catalyst, ACS Catal. (2019) 1662–1669.
[19] K.N. Houk, P.H.Y. Cheong, Computational prediction of small-molecule catalysts, Nature 455 (7211) (2008) 309–313.
[20] S. Kundu, Y. Choliy, G. Zhuo, R. Ahuja, T.J. Emge, R. Warmuth, M. Brookhart, K. Krogh-Jespersen, A.S. Goldman, Rational design and synthesis of highly active pincer-iridium catalysts for alkane dehydrogenation, Organometallics 28 (18) (2009) 5432–5444.
[21] S.L. Qu, H.G. Dai, Y.F. Dang, C.Y. Song, Z.X. Wang, H.R. Guan, Computational mechanistic study of Fe-catalyzed hydrogenation of esters to alcohols: improving catalysis by accelerating precatalyst activation with a Lewis base, ACS Catal. 4 (12) (2014) 4377–4388.
[22] S.Q. Niu, M.B. Hall, Theoretical studies of inorganic and-organometallic reaction mechanisms. 15. Catalytic alkane dehydrogenation by iridium(III) complexes, J. Am. Chem. Soc. 121 (16) (1999) 3992–3999.
[23] S. Li, M.B. Hall, Theoretical studies of inorganic and organometallic reaction mechanisms. 18. Catalytic transfer dehydrogenation of alkanes by an iridium(III) pincer complex, Organometallics 20 (11) (2001) 2153–2160.
[24] K. Krogh-Jespersen, M. Czerw, K. Zhu, B. Singh, M. Kanzelberger, N. Darji, P.D. Achord, K.B. Renkema, A.S. Goldman, Combined computational and experimental study of substituent effects on the thermodynamics of H_2, CO, arene, and alkane addition to iridium, J. Am. Chem. Soc. 124 (36) (2002) 10797–10809.
[25] K.-W. Huang, J.H. Han, C.B. Musgrave, E. Fujita, carbon dioxide reduction by pincer rhodium η^2-dihydrogen complexes: hydrogen-binding modes and mechanistic studies by density functional theory calculations, Organometallics 26 (2007) 508–513.
[26] J. Li, Y. Shiota, K. Yoshizawa, Metal-ligand cooperation in H_2 production and H_2O decomposition on a Ru(II) PNN complex: the role of ligand dearomatization-aromatization, J. Am. Chem. Soc. 131 (38) (2009) 13584–13585.
[27] M.S.G. Ahlquist, Iridium catalyzed hydrogenation of CO_2 under basic conditions-mechanistic insight from theory, J. Mol. Catal. A 324 (1–2) (2010) 3–8.
[28] Y. Chen, W.H. Fang, Mechanism for the light-induced O_2 evolution from H_2O promoted by Ru(II) PNN complex: a DFT study, J. Phys. Chem. A 114 (37) (2010) 10334–10338.
[29] T.J. Schmeier, N. Hazari, C.D. Incarvito, J.A. Raskatov, Exploring the reactions of CO_2 with PCP supported nickel complexes, Chem. Commun. 47 (6) (2011) 1824–1826.
[30] T. Debnath, T. Ash, A. Ghosh, S. Sarkar, A.K. Das, Exploration of unprecedented catalytic dehydrogenation mechanism of methylamine-water mixture in presence of Ru-pincer complex: a systematic DFT study, J. Catal. 363 (2018) 164–182.
[31] C.A. Tolman, Steric effects of phosphorus ligands in organometallic chemistry and homogeneous catalysis, Chem. Rev. 77 (3) (1977) 313–348.
[32] A. Choualeb, A.J. Lough, D.G. Gusev, Hydridic rhenium nitrosyl complexes with pncer-type PNP ligands, Organometallics 26 (14) (2007) 3509–3515.
[33] R. Tanaka, M. Yamashita, K. Nozaki, Catalytic hydrogenation of carbon dioxide using Ir(III)-pincer complexes, J. Am. Chem. Soc. 131 (2009) 14168–14169.
[34] K. Namura, H. Suzuki, Synthesis, structure, and reactivity of mixed-ligand dinuclear ruthenium polyhydrido complexes supported by 1,4,7-trimethyl-1,4,7-triazacyclononane and bulky phosphine ligands, Organometallics 33 (12) (2014) 2968–2983.
[35] M. Feller, U. Gellrich, A. Anaby, Y. Diskin-Posner, D. Milstein, Reductive cleavage of CO_2 by metal-ligand-cooperation mediated by an iridium pincer complex, J. Am. Chem. Soc. 138 (20) (2016) 6445–6454.
[36] N.S. Lambic, C.P. Lilly, R.D. Sommer, E.A. Ison, Mechanism for the reaction of CO with oxorhenium hydrides: migratory insertion of CO into rhenium hydride and formyl bonds leads to migration from rhenium to the oxo ligand, Organometallics 35 (2016) 3060–3068.
[37] T.T. Lekich, J.B. Gary, S.M. Bellows, T.R. Cundari, L.M. Guard, D.M. Heinekey, H2 addition to (Me4PCP)Ir(CO): studies of the isomerization mechanism, Dalton Trans. 47 (45) (2018) 16119–16125.
[38] X.Y. Lv, F. Huang, Y.B. Wu, G. Lu, Origin of ligand effects on reactivities of pincer-Pd catalyzed hydrocarboxylation of allenes and alkenes with formate salts: a computational study, Catal. Sci. Technol. 8 (11) (2018) 2835–2840.
[39] K.S. Sandhya, C.H. Suresh, Water splitting promoted by a ruthenium(II) PNN complex: an alternate pathway through a dihydrogen complex for hydrogen production, Organometallics 30 (14) (2011) 3888–3891.
[40] D.M. Spasyuk, S.I. Gorelsky, A. van der Est, D. Zargarian, Characterization of divalent and trivalent species generated in the chemical and electrochemical oxidation of a dimeric pincer complex of nickel, Inorg. Chem. 50 (6) (2011) 2661–2674.
[41] H. Ryu, J. Park, H.K. Kim, J.Y. Park, S.-T. Kim, M.-H. Baik, Pitfalls in computational modeling of chemical reactions and how to avoid them, Organometallics (2018).
[42] M.S. Newman, A notation for the study of certain stereochemical problems, J. Chem. Educ. 32 (1955) 344–347.
[43] T. Foldes, A. Madarasz, A. Revesz, Z. Dobi, S. Varga, A. Hamza, P.R. Nagy, P.M. Pihko, I. Papai, Stereocontrol in diphenyiprolinol silyl ether catalyzed Michael additions: steric shielding or Curtin-Hammett scenario?, J Am. Chem. Soc. 139 (47) (2017) 17052–17063.
[44] T. Husch, D. Seebach, A.K. Beck, M. Reiher, Rigorous conformational analysis of pyrrolidine enamines with relevance to organocatalysis, Helv. Chim. Acta 100 (10) (2017), e1700182-1-17.
[45] T. Kamachi, K. Yoshizawa, Low-mode conformational search method with semiempirical quantum mechanical calculations: application to enantioselective organocatalysis, J. Chem. Inf. Model 56 (2) (2016) 347–353.
[46] T. Kamachi, K. Yoshizawa, Enantioselective alkylation by binaphthyl chiral phase-transfer catalysts: a DFT-based conformational analysis, Org. Lett. 16 (2) (2014) 472–475.
[47] C.Q. He, A. Simon, Y.H. Lam, A.P.J. Brunskill, N. Yasuda, J.J. Tan, A.M. Hyde, E.C. Sherer, K.N. Houk, Model for the enantioselectivity of asymmetric intramolecular alkylations by bis-quaternized cinchona alkaloid-derived catalysts, J. Org. Chem. 82 (16) (2017) 8645–8650.
[48] D. Lehnherr, D.D. Ford, A.J. Bendelsmith, C.R. Kennedy, E.N. Jacobsen, Conformational control of chiral amido-thiourea catalysts enables improved activity and enantioselectivity, Org. Lett. 18 (13) (2016) 3214–3217.
[49] M. Käß, A. Friedrich, M. Drees, S. Schneider, Ruthenium complexes with cooperative PNP ligands: bifunctional catalysts for the dehydrogenation of ammonia-borane, Angew. Chem. Int. Edit. 48 (5) (2009) 905–907.
[50] D. Benito-Garagorri, L.G. Alves, L.F. Veiros, C.M. Standfest-Hauser, S. Tanaka, K. Mereiter, K. Kirchner, Kinetically controlled formation of octahedral trans-dicarbonyl iron(II) PNP pincer complexes: the decisive role of spin-state changes, Organometallics 29 (21) (2010) 4932–4942.
[51] D. Bacciu, C.-H. Chen, P. Surawatanawong, B.M. Foxman, O.V. Ozerov, High-spin manganese(II) complexes of an amido/bis (phosphine) PNP ligand, Inorg. Chem. 49 (11) (2010) 5328–5334.

[52] O. Blacque, C.M. Frech, Pincer-type Heck catalysts and mechanisms based on Pd^{IV} intermediates: a computational study, Chem. Eur. J. 16 (2010) 1521–1531.
[53] X.Z. Yang, Unexpected direct reduction mechanism for hydrogenation of ketones catalyzed by Iron PNP pincer complexes, Inorg. Chem. 50 (24) (2011) 12836–12843.
[54] L.C. Liang, C.W. Li, P.Y. Lee, C.H. Chang, H.M. Lee, A terminal nickel(II) anilide complex featuring an unsymmetrically substituted amido pincer ligand: synthesis and reactivity, Dalton Trans. 40 (35) (2011) 9004–9011.
[55] N. Gorgas, B. Stoger, L.F. Veiros, E. Pittenauer, G. Allmaier, K. Kirchner, Efficient hydrogenation of ketones and aldehydes catalyzed by well-defined iron(II) PNP pincer complexes: evidence for an insertion mechanism, Organometallics 33 (23) (2014) 6905–6914.
[56] J. Kothandaraman, M. Czaun, A. Goeppert, R. Haiges, J.P. Jones, R.B. May, G.K.S. Prakash, G.A. Olah, Amine-free reversible hydrogen storage in formate salts catalyzed by ruthenium pincer complex without pH control or solvent change, Chemsuschem 8 (8) (2015) 1442–1451.
[57] H. Jiao, K. Junge, E. Alberico, M. Beller, A comparative computationally study about the defined M(II) pincer hydrogenation catalysts (M = Fe, Ru, Os), J. Comput. Chem. 37 (2015) 168–176.
[58] J. Pecak, M. Glatz, B. Stoger, R. Bittner, H. Hoffmann, A. Atkins, L. Gonzalez, K. Kirchner, Visible light-induced cis/trans isomerization of dicarbonyl Fe(II) PNP pincer complexes, Polyhedron 143 (2018) 94–98.
[59] J.F. Sonnenberg, K.Y. Wan, P.E. Sues, R.H. Morris, Ketone asymmetric hydrogenation catalyzed by P-NH-P ' pincer iron catalysts: an experimental and computational study, Acs Catal. 7 (1) (2017) 316–326.
[60] J.A. Luque-Urrutia, M. Solà, D. Milstein, A. Poater, Mechanism of the manganese-pincer-catalyzed acceptorless dehydrogenative coupling of nitriles and alcohols, J. Am. Chem. Soc. (2019).
[61] R. Huber, A. Passera, A. Mezzetti, Iron(II)-catalyzed hydrogenation of acetophenone with a chiral, pyridine-based PNP pincer ligand: support for an outer-sphere mechanism, Organometallics 37 (3) (2018) 396–405.
[62] G.R. Morello, K.H. Hopmann, A dihydride mechanism can explain the intriguing substrate selectivity of iron-PNP-mediated hydrogenation, Acs Catal. 7 (9) (2017) 5847–5855.
[63] X. Yang, M.B. Hall, Mechanism of water splitting and oxygen–oxygen bond formation by a mononuclear ruthenium complex, J. Am. Chem. Soc. 132 (1) (2009) 120–130.
[64] J.W. Steed, Interplay of non-covalent bonds: effect of crystal structure on molecular structure, in: E.R.T. Tiekink, J.J. Vittal (Eds.), Frontiers in Crystal Engineering, John Wiley & Sons, Ltd, 2006.
[65] E.R.T. Tiekink, Influence of crystal structure on molecular structure: syntactic structural chemistry, Rigaku J. 19 (1) (2002) 14–24.
[66] M. Besora, A.A.C. Braga, G. Ujaque, F. Maseras, A. Lledos, The importance of conformational search: a test case on the catalytic cycle of the Suzuki-Miyaura cross-coupling, Theor. Chem. Acc. 128 (4–6) (2011) 639–646.
[67] D. Balcells, G. Drudis-Sole, M. Besora, N. Dolker, G. Ujaque, F. Maseras, A. Lledos, Some critical issues in the application of quantum mechanics/molecular mechanics methods to the study of transition metal complexes, Faraday Discuss. 124 (2003) 429–441.
[68] J. Bartol, P. Comba, M. Melter, M. Zimmer, Conformational searching of transition metal compounds, J. Comput. Chem. 20 (14) (1999) 1549–1558.
[69] V. Pandarus, D. Zargarian, New pincer-type diphosphinito (POCOP) complexes of nickel, Organometallics 26 (17) (2007) 4321–4334.
[70] S. Chakraborty, J.A. Krause, H. Guan, Hydrosilylation of aldehydes and ketones catalyzed by nickel PCP-pincer hydride complexes, Organometallics 28 (2009) 582–586.
[71] S. Chakraborty, Y.J. Patel, J.A. Krause, H. Guan, Catalytic properties of nickel bis(phosphinite) pincer complexes in the reduction of CO_2 to methanol derivatives, Polyhedron 32 (1) (2012) 30–34.
[72] Y. Wang, B. Zheng, Y. Pan, C. Pan, L. He, K.W. Huang, C-H and H-H bond activation via ligand dearomatization/rearomatization of a PNP-rhodium(i) complex, Dalton Trans. 44 (2015) 15111–15115.
[73] J.-P. Ebejer, G.M. Morris, C.M. Deane, Freely available conformer generation methods: how good are they?, J. Chem. Inf. Model. 52 (5) (2012) 1146–1158.
[74] N.O. Friedrich, C.D. Kops, F. Flachsenberg, K. Sommer, M. Rarey, J. Kirchmair, Benchmarking commercial conformer ensemble generators, J. Chem. Inf. Model. 57 (11) (2017) 2719–2728.
[75] Y.F. Guan, V.M. Ingman, B.J. Rooks, S.E. Wheeler, AARON: an automated reaction optimizer for new catalysts, J. Chem. Theory Comput. 14 (10) (2018) 5249–5261.
[76] Y. Minenkov, D.I. Sharapa, L. Cavallo, Application of semiempirical methods to transition metal complexes: fast results but hard-to-predict accuracy, J. Chem. Theory Comput. 14 (7) (2018) 3428–3439.
[77] M.J. Frisch, G.W. Trucks, H.B. Schlegel, G.E. Scuseria, M.A. Robb, J.R. Cheeseman, G. Scalmani, V. Barone, B. Mennucci, G.A. Petersson, H. Nakatsuji, M. Caricato, X. Li, H.P. Hratchian, A.F. Izmaylov, J. Bloino, G. Zheng, J.L. Sonnenberg, M. Hada, M. Ehara, K. Toyota, R. Fukuda, J. Hasegawa, M. Ishida, T. Nakajima, Y. Honda, O. Kitao, H. Nakai, T. Vreven, J.A. Montgomery Jr., J.E. Peralta, F. Ogliaro, M.J. Bearpark, J. Heyd, E.N. Brothers, K.N. Kudin, V.N. Staroverov, R. Kobayashi, J. Normand, K. Raghavachari, A.P. Rendell, J.C. Burant, S.S. Iyengar, J. Tomasi, M. Cossi, N. Rega, N.J. Millam, M. Klene, J.E. Knox, J.B. Cross, V. Bakken, C. Adamo, J. Jaramillo, R. Gomperts, R.E. Stratmann, O. Yazyev, A.J. Austin, R. Cammi, C. Pomelli, J.W. Ochterski, R. L. Martin, K. Morokuma, V.G. Zakrzewski, G.A. Voth, P. Salvador, J.J. Dannenberg, S. Dapprich, A.D. Daniels, Ö. Farkas, J.B. Foresman, J.V. Ortiz, J. Cioslowski, D.J. Fox, Gaussian 09, Gaussian Inc., Wallingford, CT, USA, 2009.
[78] A.D. Becke, Density-functional thermochemistry. 3. The role of exact exchange, J. Chem. Phys. 98 (7) (1993) 5648–5652.
[79] W.Z. Lai, J.N. Yao, S. Shaik, H. Chen, Which density functional is the best in computing C-H activation energies by pincer complexes of late platinum group metals?, J. Chem. Theory. Comput. 8 (9) (2012) 2991–2996.
[80] T. Sperger, I.A. Sanhueza, I. Kalvet, F. Schoenebeck, Computational studies of synthetically relevant homogeneous organometallic catalysis involving Ni, Pd, Ir, and Rh: an overview of commonly employed DFT methods and mechanistic insights, Chem. Rev. 115 (17) (2015) 9532–9586.
[81] L. Goerigk, A. Hansen, C. Bauer, S. Ehrlich, A. Najibi, S. Grimme, A look at the density functional theory zoo with the advanced GMTKN55 database for general main group thermochemistry, kinetics and noncovalent interactions, Phys. Chem. Chem. Phys. 19 (48) (2017) 32184–32215.
[82] N. Mardirossian, M. Head-Gordon, Thirty years of density functional theory in computational chemistry: an overview and extensive assessment of 200 density functionals, Mol. Phys. 115 (19) (2017) 2315–2372.
[83] P.J. Hay, W.R. Wadt, Ab initio effective core potentials for molecular calculations. Potentials for K to Au including the outermost core orbitals, J. Chem. Phys. 82 (1) (1985) 299–310.
[84] W.R. Wadt, P.J. Hay, Ab initio effective core potentials for molecular calculations. Potentials for main group elements Na to Bi, J. Chem. Phys. 82 (1) (1985) 284–298.

[85] P.J. Hay, W.R. Wadt, Ab initio effective core potentials for molecular calculations. Potentials for the transition metal atoms Sc to Hg, J. Chem. Phys. 82 (1) (1985) 270–283.
[86] R. Ditchfield, W.J. Hehre, J.A. Pople, Self-consistent molecular-orbital methods. IX. An extended gaussian-type basis for molecular-orbital studies of organic molecules, J. Chem. Phys. 54 (2) (1971) 724–728.
[87] W.J. Hehre, R. Ditchfield, J.A. Pople, Self-consistent molecular-orbital methods. 12. Further extensions of gaussian-type basis sets for use in molecular-orbital studies of organic-molecules, J. Chem. Phys. 56 (5) (1972) 2257-+.
[88] P.C. Harihara, J.A. Pople, Influence of polarization functions on molecular-orbital hydrogenation energies, Theor. Chim. Acta 28 (3) (1973) 213–222.
[89] C.T. Lee, W.T. Yang, R.G. Parr, Development of the Colle-Salvetti correlation-energy formula into a functional of the electron-density, Phys. Rev. B 37 (2) (1988) 785–789.
[90] C. Zhou, J. Hu, Y. Wang, C. Yao, P. Chakraborty, H. Li, C. Guan, M.-H. Huang, K.-W. Huang, Selective carbonylation of benzene to benzaldehyde using a phosphorus–nitrogen PN3P–rhodium(i) complex, Org. Chem. Front. 6 (6) (2019) 721–724.
[91] V.M. Rayon, J.A. Sordo, Pseudorotation motion in tetrahydrofuran: an ab initio study, J. Chem. Phys. 122 (20) (2005) 204303.
[92] X. Lefevre, G. Durieux, S. Lesturgez, D. Zargarian, Addition of amines and phenols to acrylonitrile derivatives catalyzed by the POCOP-type pincer complex [{κ^{P}-κ^{C}, $^{\kappa}$P-2,6-(i-P$_r$2PO$_j$)2$_C$6$_H$3}Ni(NCMe)][OS$_O$2C$_F$3], J. Mol. Catal. A 335 (1–2) (2011) 1–7.
[93] Q.Q. Ma, T. Liu, S.J. Li, J. Zhang, X.N. Chen, H.R. Guan, Highly efficient reduction of carbon dioxide with a borane catalyzed by bis(phosphinite) pincer ligated palladium thiolate complexes, Chem. Commun. 52 (99) (2016) 14262–14265.
[94] T. Liu, W.J. Meng, Q.Q. Ma, J. Zhang, H.Z. Li, S.J. Li, Q.Y. Zhao, X.N.A. Chen, Hydroboration of CO2 catalyzed by bis(phosphinite) pincer ligated nickel thiolate complexes, Dalton Trans. 46 (14) (2017) 4504–4509.
[95] J. Zhang, J.R. Chang, T. Liu, B.L. Cao, Y.Z. Ding, X.N. Chen, Application of POCOP pincer nickel complexes to the catalytic hydroboration of carbon dioxide, Catalysts 8 (2018) (11).
[96] N.A. Eberhardt, N.P.N. Wellala, Y. Li, J.A. Krause, H. Guan, Dehydrogenative coupling of aldehydes with alcohols catalyzed by a nickel hydride complex, Organometallics (2019).
[97] F. Liu, E.B. Pak, B. Singh, C.M. Jensen, A.S. Goldman, Dehydrogenation of n-alkanes catalyzed by iridium "pincer" complexes: regioselective formation of r-olefins, J. Am. Chem. Soc. 121 (1999) 4086–4087.
[98] A. Paul, C.B. Musgrave, Catalyzed dehydrogenation of ammonia-borane by iridium dihydrogen pincer complex differs from ethane dehydrogenation, Angew. Chem. Int. Edit. 46 (43) (2007) 8153–8156.
[100] GenRot - Software to generate rotamers of molecules from Gaussian input files. 2019.